NUMERICAL ANALYSIS OF THE PROCESSES OF HEATING AND CONVECTIVE EVAPORATION OF METAL IN PULSE LASER TREATMENT

I.V. KRIVTSUN, I.L. SEMYONOV and **V.F. DEMCHENKO**
E.O. Paton Electric Welding Institute, NASU, Kiev, Ukraine

Mathematical model of the processes of heating, melting and evaporation of metal under the effect of a focused laser beam is suggested. The model allows describing thermal processes in the bulk of metal and gas-dynamic processes in a metal vapour flow occurring in laser treatment by using pulse lasers. Numerical analysis was conducted to study the processes of heating and convective evaporation of metal with a millisecond pulse of the Nd:YAG-laser beam affecting a low-carbon steel sample.

Keywords: *pulse laser, laser radiation, metal, temperature field, evaporation, metal vapour, Knudsen layer, gas-dynamic processes, mathematical model*

Investigation of physical processes occurring in interaction of the high-intensity laser beam with a material plays an important role in development of new technologies for laser welding and treatment of different materials, and first of all the metallic ones [1–4]. Of special interest for upgrading of such technologies as microwelding, engraving, drilling, etc. is investigation into the processes of interaction of the focused pulse and pulse-periodic laser beams with metals [5–8]. Such processes include absorption of the laser beam by metal, its heating, melting and subsequent evaporation accompanied by scattering of the metal vapour into a surrounding gas (convective evaporation mode). Normally, analysis of convective evaporation of metal to determine quantitative characteristics of the evaporation process (density, temperature and velocity of scattering of the vapour) is performed by using a model suggested by C. Knight [9]. This model is based on the assumptions that the vapour flow is unidimensional and stationary. However, both of the above assumptions are known to be invalid in a case of high-rate heating of metal with a focused pulse laser beam, as upon reaching boiling temperature T_b the melt surface at the heat spot centre continues heating up to the temperatures that are much in excess of T_b, and the vapour flowing from the heat spot experiences side unloading, this causing violation of the unidimensional flow pattern assumed in study [9]. The present study is aimed at analysis of applicability of different models describing convective evaporation of metal under the conditions of heating of a metal plate with the focused pulse laser beam (ionisation of vapour and formation of laser plasma being ignored).

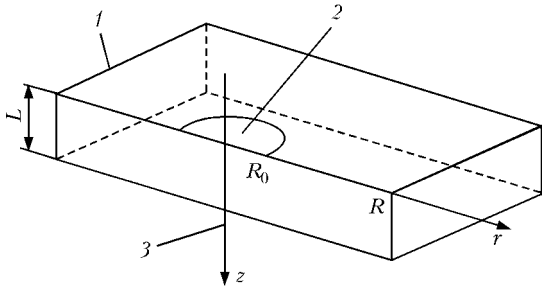

Figure 1. Scheme of heating of metal plate by laser beam: *1* — plate; *2* — heat spot; *3* — laser beam axis

Consider the process of heating of a metal plate with single pulse of the focused laser beam. Assuming the spatial distribution of the radiation intensity to be symmetric about the beam axis, formulate the mathematical model of heating of the plate in the axisymmetric statement. Introduce the cylindrical coordinate system as shown in Figure 1. Assume that radiation intensity I_0 is distributed uniformly over the heat spot with radius R_0 and remains constant during the pulse. Radiation intensity I_0 is determined through total energy W of the pulse, its duration τ and cross section area of the beam on the plate surface, $S = \pi P_0^2$, as follows: $I_0 = W/(\tau S)$.

The volumetric character of absorption of laser radiation can be ignored for the majority of metals. Then the thermal effect by the laser beam on a metal sample can be assumed to be a surface heat source distributed over the plate surface with density $q(r)$:

$$q(r) = \begin{cases} A(T_s)I_0 & \text{at } r \le R_0, \\ 0 & \text{at } r > R_0, \end{cases} \qquad (1)$$

where $A(T_s)$ is the coefficient of absorption of laser radiation, which depends upon the temperature on the metal surface, $T_s(r)$.

Write down the equation of thermal conductivity of a sample in the following form:

$$C(T)\rho(T)\frac{\partial T}{\partial t} = \frac{1}{r}\frac{\partial}{\partial r}\left(r\lambda(T)\frac{\partial T}{\partial r}\right) + \frac{\partial}{\partial z}\left(\lambda(T)\frac{\partial T}{\partial z}\right), \quad 0 < r < R, \quad 0 < z < L, \quad t > 0, \qquad (2)$$

where $C(T)$, $\rho(T)$ and $\lambda(T)$ are, respectively, the effective heat capacity of metal (allowing for the latent melting heat), density and coefficient of thermal conductivity.

Write down the boundary conditions for equation (2) in the following form:

$$\frac{\partial T}{\partial r}\Big|_{r=0} = 0; \quad T(r, L, t) = T(R, z, t) = T_0;$$
$$-\lambda(T_s)\frac{\partial T}{\partial z}\Big|_{z=0} = q - q_{rc} - q_e. \tag{3}$$

Here $q_{rc}(T_s) = \varepsilon\sigma(T_s^4 - T_0^4) + \alpha(T_s - T_0)$ are the losses of heat for radiation and heat exchange between the surface and environment; ε is the emissivity factor of the metal surface; σ is the Stefan–Boltzmann constant; α is the heat exchange coefficient; T_0 is the ambient temperature; $q_e(T_s) = \kappa q_m(T_s)$ is the specific heat flow carried away by the vapour from the melt surface; κ is the specific vaporization heat; $q_m(T_s) = \overline{\rho u}$ is the specific mass flow of the vapour; $\overline{\rho}$ and $\overline{u}$ are, respectively, the density and velocity of the metal vapour near the evaporating surface.

To close problems (2) and (3), it is necessary to use the model of convective evaporation of metal, allowing calculation of velocity $\overline{u}$ and density $\overline{\rho}$. Within the framework of the Knight's model, structure of the unidimensional subsonic flow of the vapour can be described as follows (Figure 2): the shock wave propagates via an ambient gas, followed by a contact discontinuity that is a contact region between the ambient gas and expanding metal vapour.

The Knudsen layer with thickness of an order of several lengths of the free path exists near the evaporating metal surface, outside which (in the gas-dynamic flow region) the equilibrium is established on translational degrees of freedom of the vapour particles. Study [9] suggests the following dependencies relating density $\overline{\rho}$ and temperature $\overline{T}$ of the vapour at the Knudsen layer boundary to saturated vapour density ρ_s and evaporating surface temperature T_s:

$$\frac{\overline{T}}{T_s} = \left[\sqrt{1 + \pi\left(\frac{\gamma-1}{\gamma+1}\frac{m}{2}\right)^2} - \sqrt{\pi}\,\frac{\gamma-1}{\gamma+1}\frac{m}{2}\right]^2, \tag{4}$$

$$\frac{\overline{\rho}}{\rho_s} = \sqrt{\frac{T_s}{\overline{T}}}\left[\left(m^2 + \frac{1}{2}\right)e^{m^2}\operatorname{erfc}(m) - \frac{m}{\sqrt{\pi}}\right] + \frac{1}{2}\frac{T_s}{\overline{T}}\left[1 - \sqrt{\pi}\, m e^{m^2}\operatorname{erfc}(m)\right]. \tag{5}$$

Here $m = \overline{u}/\sqrt{2\Re\overline{T}} = \sqrt{\gamma/2}\overline{\mathrm{M}}$; $\Re$ is the gas constant; $\gamma = 5/3$ is the adiabatic exponent of the vapour, which is assumed to be a monatomic ideal gas; and $\overline{\mathrm{M}}$ is the Mach number at the Knudsen layer boundary.

Pressure of the saturated vapour can be found from the Clausius–Clayperon equation, and density — from the equation of state of the ideal gas, $\overline{p} = \rho\Re\overline{T}$. Velocity $\overline{u}$ and pressure $\overline{p}$ are related to density ρ_0 and pressure in the ambient gas through the shock wave relationship [9]

$$\overline{u} = \frac{\overline{p} - p_0}{\sqrt{\frac{\rho_0}{2}(\overline{p}(\gamma+1) + p_0(\gamma-1))}}. \tag{6}$$

One non-linear equation for determination of velocity $\overline{u}$ can be derived from relationships (4) through (6) (the possibility of using conjugate model (2)–(6) is limited by the Knight assumption of the stationary character of the vapour flow).

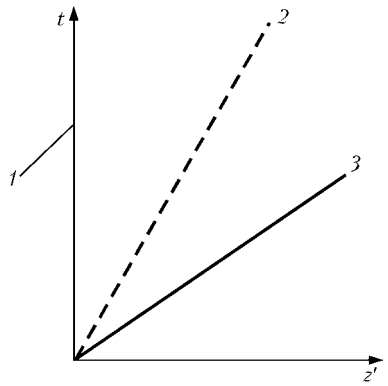

Figure 2. Scheme of unidimensional scattering of vapour [9]: *1* — Knudsen layer; *2* — contact discontinuity; *3* — shock wave

Consider the problem of non-stationary gas dynamics of the metal vapour by keeping, as earlier, to the assumption of a unidimensional flow pattern. Let Oz' be the axis of the cylindrical coordinate system, which is directed normal to the plate surface towards the vapour phase. At a high Reynolds number (velocity of scattering of the vapour is of an order of 500–700 m/s), the Euler equation can be used to describe gas-dynamics of the vapour-gas mixture:

$$\frac{\partial \mathbf{U}}{\partial t} + \frac{\partial \mathbf{F}}{\partial z'} = 0, \quad z' \in [0, H], \tag{7}$$

where $\mathbf{U} = (\rho_m, \rho, \rho_u, E)$; $\mathbf{F} = (\rho_m u, \rho u, \rho u^2 + p)$; $(E + p)u)$; ρ, u and p are the density, velocity and pressure of the mixture, respectively; ρ_m is the density of the metal vapour; $E = \rho e + \rho u^2/2$ is the energy of the mixture; and $e = p/\rho(\gamma - 1)$ is the internal energy.

Integrate equation (7) with respect to the following boundary and initial conditions:

$$\frac{\partial \mathbf{U}}{\partial z'}\Big|_{z'=H} = 0, \quad t > 0, \tag{8}$$

$$u(0, t) = u_{0+} + \frac{p(0, t) - p_{0+}}{\sqrt{\frac{\rho_{0+}}{2}[p(0, t)(\gamma+1) + p_{0+}(\gamma-1)]}},$$
$$\rho_m(0, t) = \rho(0, t), \quad p(0) = p(0, t)RT, \quad t \geq 0; \tag{9}$$

$$p(z', 0) = p_0, \; u(z', 0) = 0, \quad \rho(z', 0) = \rho_0, \quad \rho_m(z', 0) = 0, \quad 0 < z' < H, \tag{10}$$

where $p_{0+} = p(+0, t)$; $\rho_{+0} = \rho(+0, t)$ and $u_{+0} = u(+0, t)$.

Density ρ and temperature T at $z' = 0$ and $t \geq 0$ are determined from conditions (4) and (5), assuming that $\overline{\rho} = \rho$, $\overline{T} = T$, and $\overline{u} = u(0, t)$.

The Peacemen–Rachford method [10] with local non-linearity iterations in difference analogue of the condition of local energy balance on the plate surface was used to find numerical solution for problem (2) and (3). The problem of non-stationary gas dynamics (7) through (10) was solved by the Godunov method of the second order of accuracy [11].

Consider heating of the low-carbon steel plate with single pulse of the focused laser beam having the following parameters: $I_0 = 5\cdot10^6$ W/cm^2, $\tau = 1$ ms, and $R_0 = 0.1$ mm. This corresponds, e.g. to characteristic

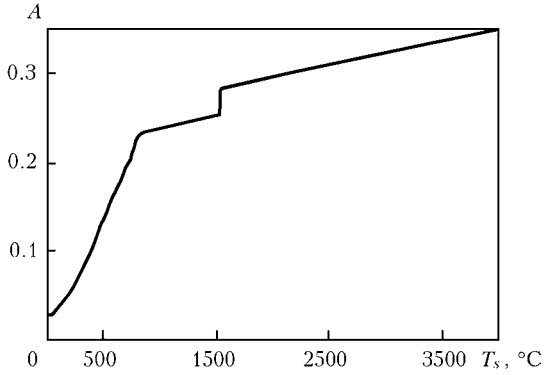

Figure 3. Temperature dependence of coefficient of absorption of Nd:YAG-laser radiation on low-carbon steel sample

operating parameters of the pulse Nd:YAG laser, which is part of the welding, cutting and deep engraving unit [12]. The following values were chosen for plate thickness L and calculation domain radius R (see Figure 1): L = 1 mm and R = 2 mm. Thermal-physical properties of low-carbon steel were taken from study [13], and corresponding temperature dependence of the coefficient of absorption of laser radiation was calculated from the data of studies [14–16] (Figure 3). Iron was used as an evaporating material, and air under normal conditions was used as an atmospheric gas.

Let us conduct comparative analysis of solution of the self-consistent problem of heating (1) through (3)

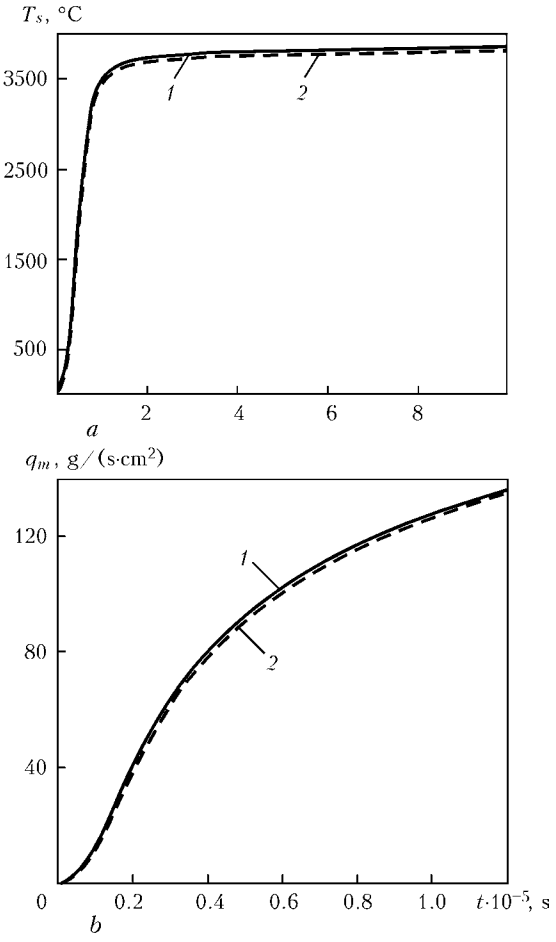

Figure 4. Dynamics of variations in metal temperature at the heat spot centre (*a*) and mass flow from the melt surface (*b*): *1* — non-stationary model; *2* — stationary model

and convective evaporation of metal for two models of gas-dynamics of the vapour: stationary [9] and non-stationary (4), (5) and (7) through (10) for a case of heating of the plate with a laser radiation pulse. The calculation results are shown in Figures 4 and 5 (the time in Figures 4, *b* and 5 is counted out from the beginning of evaporation). At the chosen parameters of the laser pulse, temperature at the centre of the heat spot reaches the boiling point during 7 μs (Figure 4, *a*), and it continues growing to 3800 °C for approximately 80 μs, after which it remains almost constant up to the end of the pulse. In a mode of stabilisation of the metal surface temperature, due to laser heating the heat flow is compensated for by the losses of heat for evaporation and, partially, by the radiant heat exchange between the surface and environment.

By the time moment (with respect to the beginning of evaporation) when the metal surface temperature stops varying with time, the shock wave has moved to a distance that is much in excess of the characteristic size of domain of the gas-dynamic problem solution (e.g. diameter of the heat spot), and no longer affects kinetics of the process of evaporation of metal from the melt surface. If the time during which the molten metal surface reaches the stationary value of temperature tends to zero (infinitely high heating rate), the gas-dynamic characteristics of the flow (velocity and pressure) correspond to the Knight model. In spite of the fact that in the non-stationary model of convective evaporation these characteristics differ from the Knight idealised flow scheme (see Figure 5), the values of the specific mass flow of the vapour at the Knudsen layer boundary calculated from the stationary and non-stationary evaporation models almost coincide (see Figure 4, *b*). This is explained by the fact that the time during which the surface reaches the stationary value of temperature (see Figure 4, *a*) is much shorter than the characteristic time of setting of the gas-dynamic processes. Therefore, it might be expected that a more substantial difference in structure of the flow and, accordingly, in value of the specific mass flow, $q_m(t)$, will occur with decrease in the heating rate.

To illustrate the last statement, consider heating of the plate with laser radiation of lower intensity $I_0 = 7\cdot10^5$ W/cm^2. In contrast to the above heating conditions, differences between the stationary and non-stationary evaporation models at low heating rates become more substantial in terms of the thermal problem solution (Figure 6). Therefore, at lower heating rates it is necessary to allow for the non-stationary character of the gas-dynamic processes.

The above models are valid for evaporation of metal with a developed liquid surface (with unlimited flat surface). In evaporation from the heat spot of a small diameter, as is the case of the focused laser beam affecting the surface, the assumption of a unidimensional structure of the gas-dynamic flow is violated. To study the effect of side scattering of the vapour, consider the two-dimensional problem of gas dynamics for a vapour-gas mixture in the axisymmetric statement. The Euler equations in the cylindrical coordinate system (r, z') have the following form:

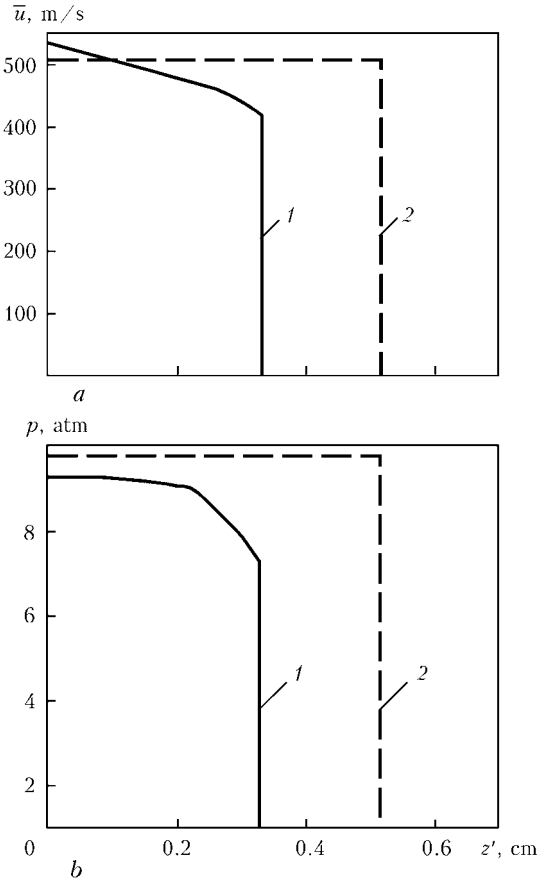

Figure 5. Distribution of velocity of vapour (*a*) and gas-dynamic pressure (*b*) in vapour phase at $t = 6.7 \cdot 10^{-6}$ s: *1*, *2* — same as in Figure 4

$$\frac{\partial \mathbf{U}}{\partial t} + \frac{\partial \mathbf{F}}{\partial r} + \frac{\partial \mathbf{G}}{\partial z'} = -\frac{\mathbf{f}}{r}. \qquad (11)$$

Here $\mathbf{U} = (\rho_1, \rho, \rho u, \rho v, E)$; $\mathbf{f} = (\rho_1 u, \rho u, \rho u, (E + p)u)$; $\mathbf{F} = (\rho_m u, \rho u, \rho u^2 + p, \rho uv, (E + p)u)$; $\mathbf{G} = (\rho_m v, \rho v, \rho uv, \rho v^2 + p, (E + p)v)$; u and v are the axial and radial components of the velocity vector, respectively; $E = \rho e + (\rho u^2 + \rho v^2)/2$ is the mixture energy; and $e = p/\rho(\gamma - 1)$.

Integrate equation (11) in a domain shown in Figure 7.

Boundaries Γ_4 and Γ_5 are the external boundaries of the flow region, Γ_3 is the symmetry axis, and Γ_6 is the metal surface outside the evaporation spot. The Knudsen layer on the surface of the liquid metal pool is modelled by a rectangular protrusion with boundaries Γ_1 and Γ_2. The boundary condition similar to (9) is set at boundary Γ_1. Tangential component of the velocity vector at this boundary is redefined from the flow region by the characteristic relationships. The non-flow boundary condition is set on the metal surface, symmetry condition is set on the flow axis, and non-reflection boundary conditions are set at external boundaries Γ_4 and Γ_5. The initial conditions are set to be as follows: $p = p_0$, $u = 0$, $v = 0$, $\rho = \rho_0$, and $\rho_1 = 0$, where p_0 and ρ_0 are the pressure and density of the atmospheric gas.

The formulated problem of two-dimensional gas dynamics was solved by the Godunov method of the second order of accuracy (TVD scheme). Sizes of the calculation domain were chosen to be as follows: length of boundary Γ_1 was 0.015 cm, and Knudsen layer width Γ_2 was assumed to be 0.006 cm (proceeding from the estimation of mean length of the free path in the atmospheric gas and metal vapours immediately over the melt). Sizes of external boundaries Γ_5 and Γ_6 of the calculation domain were assumed to be equal to $6L_0$. Air under normal conditions was assumed to be the ambient gas, and temperature of the evaporating metal surface was assumed to be constant and equal to 4000 °C.

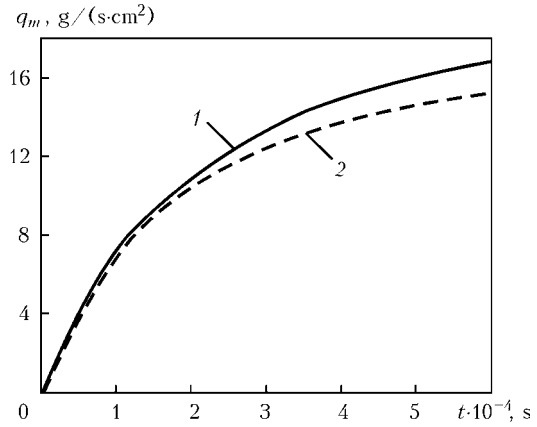

Figure 6. Time variations of mass flow of vapour at $I_0 = 7 \cdot 10^5$ W/cm^2: *1*, *2* — same as in Figure 4

The calculation results are shown in Figures 8 and 9. The qualitatively different flow pattern takes place in a case of side unloading of the vapour flow. Velocity at the Knudsen layer boundary does not reach the stationary value (like in the unidimensional case), but monotonously grows until the Mach number becomes equal to one (Figure 8, *b*). After that a stationary compression shock forms in the vapour flow region with a contact discontinuity propagating behind it at a constant velocity. The compression shock forms because pressure in a region between the Knudsen layer boundary and ambient gas becomes lower than the atmospheric one (region of decreased pressure in Figure 8, *a*). The shock wave at the time moment under consideration is at a distance of 0.075 cm from the Knudsen layer boundary, the decreased pressure region and compression shock being at a distance of 0.05 cm. Such flow pattern was fixed in [5] in investigation of the impact on metal by the pulse laser beam. It should be noted that the similar structure of

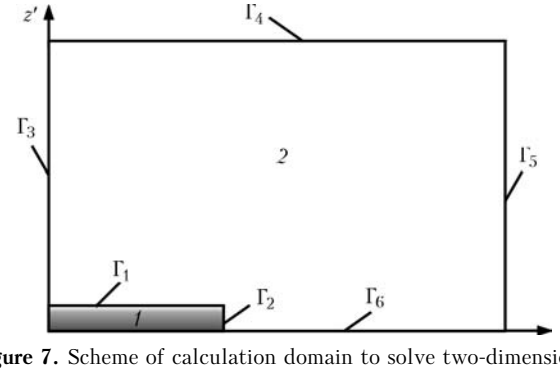

Figure 7. Scheme of calculation domain to solve two-dimensional equations of gas dynamics: *1* — Knudsen layer; *2* — gas-dynamic region

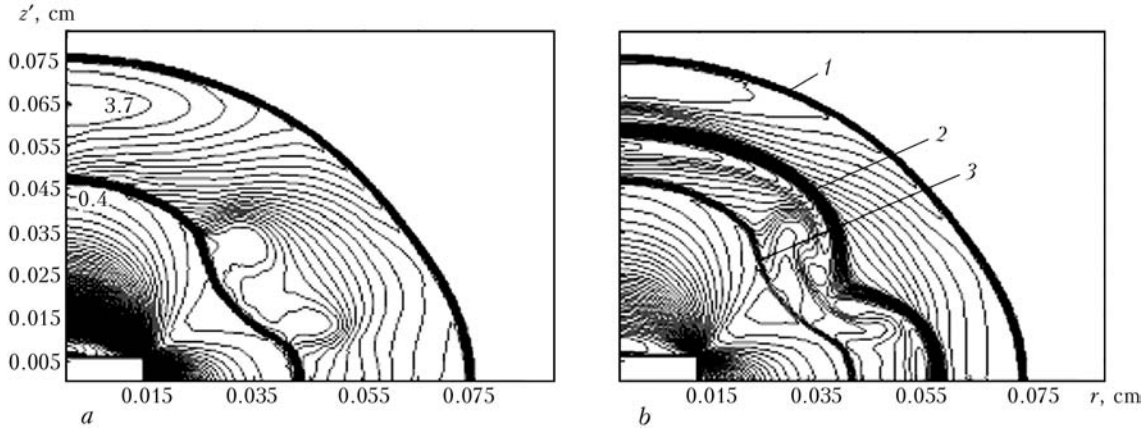

Figure 8. Isolines of pressure p/p_0 (*a*) and density (*b*) at $t = 4 \cdot 10^{-7}$ s: *1* — shock wave; *2* — contact discontinuity; *3* — compression shock

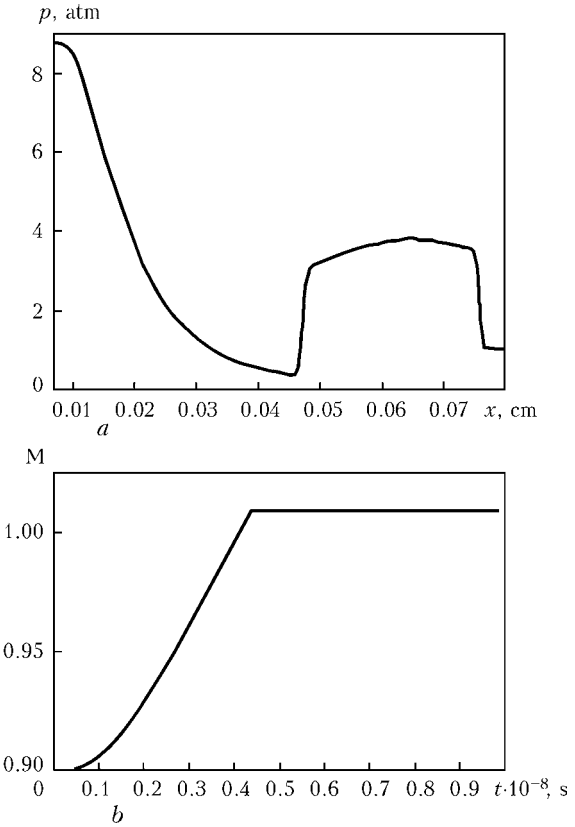

Figure 9. Distribution of pressure along the symmetry axis at $t = 4 \cdot 10^{-7}$ s (*a*) and time dependence of the maximal value of Mach number at the Knudsen layer boundary (*b*)

the flow occurs also in the case of a supersonic outflow of gas from the nozzle in a mode of underexpansion.

Consider the non-stationary conditions of heating of metal with the laser beam. The time of reaching the stationary temperature value by the surface is approximately three orders of magnitude longer than the time during which the Mach number at the Knudsen layer boundary becomes equal to one. Therefore, in the case of side unloading of the vapour the problem of metal heating with the laser beam can be solved with a sufficiently good approximation by assuming the Mach number at the Knudsen layer boundary to be equal to one. In this case, the mass flow can be found from relationships (4) and (5) without solving the gas dynamic problem.

It should be noted in conclusion that such characteristics as the thermal state of metal, density of the mass flow of the metal vapour, its scattering velocity, losses of heat for evaporation and pressure of the vapour recoil reaction, which are important in terms of technological applications, are determined not only by the conditions of metal heating, but also by the gas-dynamic processes occurring in the vapour phase. In a general case, the self-consistent model describing thermal processes in the bulk of metal and processes of heat and mass transfer in the Knudsen layer, as well as gas-dynamic processes in the vapour flow should be used to model the situation under consideration.

1. Arutyunyan, R.V., Baranov, V.Yu., Bolshov, L.A. et al. (1989) *Effect of laser radiation on materials*. Moscow: Nauka.
2. Vedenov, A.A., Gladush, G.G. (1985) *Physical processes in laser treatment of materials*. Moscow: Energoatomizdat.
3. Dulie, U. (1986) *Laser technology and analysis of materials*. Moscow: Mir.
4. *Anisimov, S.I., Imas, Ya.A., Romanov, G.S. et al.* (1970) Effect of high radiation power on metals. Moscow: Nauka.
5. Batarov, V.A., Bunkin, F.V., Prokhorov, A.M. et al. (1970) Stationary shock wave generated in stationary metal evaporation under the effect of laser radiation. *Pisma v Zhurnal Eksperim. i Teoret. Fiziki*, **11**, 113–118.
6. Gusarov, A.V., Gnedovets, A.G., Smurov, I. (2000) Gas dynamics of laser ablation: Influence of ambient atmosphere. *J. Appl. Phys.*, **88**, 4352–4364.
7. Afanasiev, Yu.V., Belenov, E.M., Krokhin, O.N. et al. (1969) Ionisation processes in laser plasma. *Pisma v Zhurnal Eksperim. i Teoret. Fiziki*, **10**, 553–557.
8. Vorobiov, V.S. (1993) Plasma generated in interaction of laser radiation with solid targets. *Ukr. Fizich. Zhurnal*, 163(**12**), 51–82.
9. Knight, C.J. (1979) Theoretical modelling of quick surface evaporation in presence of counterpressure. *Raketnaya Tekhnika i Kosmonavtika*, **5**, 81–86.
10. Peacemen, D.W., Rachford, H.H. (1955) The numerical solution of parabolic and elliptic differential equations. *J. Soc. Ind. Appl. Math.*, **3**, 28–41.
11. Kulikovsky, A.G., Pogorelov, N.V., Semyonov, A.Yu. (2001) *Mathematical problems in numerical solution of hyperbolic equation systems*. Moscow: Fizmatlit.
12. Kirichenko, V., Gryaznov, N., Krivtsun, I. (2008) Experimental facility for research on pulsed laser-microplasma welding. *The Paton Welding J.*, **8**, 26–30.
13. Hu, J., Tsai, H.L. (2007) Heat and mass transfer in gas metal arc welding. Pt 1. The arc. *Int. J. Heat and Mass Transfer*, **50**, 833–846.
14. Kikuo, U. (1972) Reflectivity of metals at high temperatures. *J. Appl. Phys.*, 43(**5**), 2376–2383.
15. Ordal, M.A., Long, L.L., Bell, R.J. et al. (1983) Optical properties of the metals Al, Co, Cu, Au, Fe, Pb, Ni, Pd, Pt, Ag, Ti and W in the infrared and far infrared. *Appl. Opt.*, 22(**7**), 1099–1119.
16. Miller, J. (1969) Optical properties of liquid metals at high temperatures. *Phil. Mag.*, 20(**12**), 1115–1132.